

# Conservation and analytical study of metallic elements from medieval Spanish stained glass windows

M. García-Heras<sup>1</sup>, M.A. Villegas<sup>1</sup>, E. Cano<sup>1</sup>, And J.M. Bastidas<sup>1</sup>; F. Cortés<sup>2</sup>  
Julio 2003

---

## Abstract

This contribution is focused on some metallic elements from the stained glass windows of the Monastery of Pedralbes, Barcelona, and the Cathedral of Seville (Spain). The main goal of the research was to assess their current state of conservation by studying microstructural features and mechanisms of corrosion. The samples were characterised through scanning electron microscopy (SEM), energy dispersive X-ray microanalysis (EDX), metallographic observations and X-ray diffraction (XRD).

Results obtained allow to conclude that lead comes presented a slight degree of deterioration. Their corrosion products are mainly composed of lead oxide, lead carbonate and lead sulphate which provide good protection to this material. On the contrary, iron support bars presented a higher degree of deterioration characterised by the occurrence of iron oxides and hydroxides which slowly corrode the material. Overall, the data achieved have been useful to make decisions for future preservation of these works of art and to approach technological aspects of ancient production.

Keyword Medieval stained windows / Lead comes / Iron supporting elements / Weathering / Conservation state.

---

## Introduction

Studies on Medieval stained glass windows are mainly concentrated on the analysis of coloured glasses and the iconographic elements painted on their surface [1-6]. However, up today little attention has been paid to other secondary but not less important elements such as lead comes, iron support bars, putties, mortars, cementing materials and so on [7-9]. H-shaped lead comes were commonly used to assemble glass pieces, due to the flexibility, ductility, low melting point, and relatively low cost of the lead [10]. These comes were soldered to each other using tin. Besides lead and tin, iron elements (called *ferramenta*) were used to support stained glass window panels to the walls.

The Monastery of Pedralbes (Barcelona, Spain), was built around 1328 A.D. It has an exceptional ensemble of stained glass windows from the beginning of the 14th century that has preserved the original Medieval lead comes. Such a network is now considered one of the oldest examples in Spain, since only the Cistercian windows in the Monastery of Santes Creus (Tarragona), from the 13th century, have conserved older lead comes [11].

The Cathedral of Seville, built between 1402 and 1519 A.D., has also preserved an important group of stained glass windows from the last quarter of the 15th century, located in the central nave of the building

---

<sup>1</sup> CENIM, National Centre for Metallurgical Research-CSIC, Avda. Gregorio del Amo 8, 28040 Madrid, Spain.

<sup>2</sup> Fundació Centre del Vidre, Comtes de Bell-lloc 192, 08014 Barcelona, Spain.

[12]. Most of these stained glass windows openings still have their original iron framework supports which are mostly composed of T-bars, saddle-bars and T-bar pins.

Recent conservation and restoration works carried out since 1999 in the Monastery of Pedralbes and since 2000 in the Cathedral of Seville have allowed the recovery of several well documented lead comes from the former and some iron supporting elements from the latter. The aim of this communication is to study these metallic materials from Spanish Medieval stained glass windows. The main goal of the research was to assess their current state of conservation by studying microstructural features and mechanisms of decay and corrosion derived from weathering exposure. The resulting data will be useful to make decisions for future restoration and conservation of such historical materials and to approach technological aspects of ancient production processes.

## **Experimental**

Three lead samples from the stained glass windows of the Monastery of Pedralbes were investigated. All of them come from the O II window, dated by stylistic, iconographic, and technical criteria between 1330 and 1350 A.D. This window, which is supposedly conserved in its original location, is attributed to an unknown author [13, 14]. Two of the samples are H-shaped lead comes (figure 1A-B), while the third one is a Dutchmen lead used to cover glass cracks (figure 1C).

Two iron framework supporting samples from the stained glass windows of the Seville's Cathedral were also investigated. These samples come from the NXIII window which, according to documentary data, was made by Enrique Alemán between 1478 and 1483 A.D. [12]. The first sample belongs to a square-shaped saddle-bar from a tracery panel (figure 1D) and the second one to a T-bar pin (figure 1E), both of them placed outside the window.

The metallographic structure and the corrosion layers formed on the samples have been investigated using optical microscopy (OM), scanning electron microscopy (SEM) combined with energy dispersive X-ray microanalyses (EDX) and X-ray diffraction (XRD).

After a first examination using an Olympus DP-11 conventional reflected light microscope, samples were cold mounted using a cold mounting epoxy resin (Epo-fix). The SEM observations were made through a Jeol JXA-840 electron microscope, with an attached Rontec EDX microanalysis system equipped with a windowless Si (Li) detector and acceleration voltages of 15 kV. Both inner and outer sides (indoor and outdoor) fresh weathered surfaces and polished resin inlaid cross section pellets were observed once coated by a conductive carbon film. Accordingly, carbon was discarded from the EDX determinations. XRD analysis of the corrosion products scrapped from the surface of the samples was performed using a Siemens D-5000 unit, using  $K\alpha$  of Cu radiation (1.54056 Å). Patterns were recorded in the step scanning mode, with a  $0.030^\circ$  ( $2\theta$ ) step and 5 s counting time.

## Results and discussion

Optical microscopy inspection of the lead samples showed the presence of many microcracks on the surface of the weathered lead. The origin of the microcracks could be related to the thermal stress produced by successive day-night/summer-winter cycles, which could induce expansion and shrinkage of the lead came network. These cycles could then originate mechanical stress since linear expansion coefficients of lead and glass are different. They could be also related to the mechanical stress caused by prolonged exposure to wind pressure. Nevertheless, additional microcracks produced during dismantling of panels cannot be discarded.

Corrosion products formed over lead samples seem to be very adherent and compact. On the other hand, OM inspection of the iron samples showed a layer of extensive and heterogeneous corrosion products, with a high porosity. Figure 2 shows a cross section of the square-shaped saddle-bar, showing cracks (zone 1) and highly porous areas (zone 2) formed by the corrosion products. Examination of the T-bar pin showed similar features.

Figure 3 shows SEM micrographs of the lead samples, from the external (Fig. 3A) and internal (Fig. 3B) surface of the samples, and two cross sections (Figs. 3C-D). EDX microanalyses of the external layer (table I, P1) show the presence of oxygen, silicon, aluminium, iron, calcium, and potassium which decrease altogether the percentage of lead (up to 23.9 wt. %); whereas in the internal layer (table I, P2) only lower concentrations of calcium and aluminium and a higher lead content (47.1 wt. %) were detected. These data suggest an stratified structure, where corrosion products such as lead oxides and lead carbonates (typical products of the atmospheric corrosion of lead) are present in the deeper layer, and this layer is covered by residual putty and/or mortar, as well as other deposits and dirtiness remains. The iron content, on the other hand, could result from the deposition of iron ions leached away from the framework supporting elements.

EDX microanalyses obtained on an inner H-side surface also showed two distinct layers, one of them dark and very porous with a high contents of calcium, oxygen and magnesium (table I, P3-P4). This layer can be attributed to putty remains concentrated on that area of the lead came, since putties were commonly composed of calcium carbonate mixed with linseed oil [11].

The stratified structure is also observed in the cross section (figure 3C). The most external layer, which appeared darker, presented a relatively compact microstructure of approximately 30  $\mu\text{m}$  in thickness, with a composition (table I, P5) similar to the outer layer of Fig. 3A. The deeper layer formed above the lead profile (figure 3C) (table I, P6), which appeared lighter and showed a porous microstructure of nearly 10  $\mu\text{m}$  in thickness, has a lower concentration of silicon, calcium, and aluminium and higher values of lead (24.4 wt. %), oxygen, and phosphorus. The presence of phosphorus in the corrosion layer can be attributed to excrements of pigeons and other birds.

Table I. EDX microanalyses of lead samples (atomic wt. %).

| Analysis | wt. % |     |     |     |      |      |      |     |     |     |      |      |     |
|----------|-------|-----|-----|-----|------|------|------|-----|-----|-----|------|------|-----|
|          | O     | Na  | Mg  | Al  | Si   | P    | Pb   | S   | Cl  | K   | Sn   | Ca   | Fe  |
| P1       | 45.1  | 0.2 | 0.8 | 8.5 | 15.6 | --   | 23.9 | --  | --  | 1.1 | --   | 1.4  | 3.4 |
| P2       | 49.0  | --  | --  | 1.2 | --   | --   | 47.1 | --  | --  | --  | --   | 2.7  | --  |
| P3       | 50.5  | 2.6 | 2.9 | 3.3 | 7.3  | --   | 12.2 | --  | --  | 1.0 | --   | 18.6 | 1.6 |
| P4       | 65.2  | 0.7 | 3.0 | 4.3 | 9.1  | --   | 1.3  | --  | --  | 1.6 | --   | 13.3 | 1.5 |
| P5       | 50.9  | 0.5 | 1.9 | 7.7 | 14.3 | 3.1  | 3.6  | --  | 1.1 | 1.1 | --   | 13.8 | 2.0 |
| P6       | 60.3  | --  | --  | 0.7 | 2.8  | 10.2 | 24.4 | --  | --  | --  | --   | 1.5  | --  |
| P7       | 34.8  | --  | --  | --  | --   | --   | 65.2 | --  | --  | --  | --   | --   | --  |
| P8       | --    | --  | --  | --  | 1.3  | --   | --   | --  | --  | --  | 98.7 | --   | --  |
| P9       | 48.6  | --  | --  | --  | --   | --   | 44.9 | --  | --  | --  | 6.5  | --   | --  |
| P10      | 81.3  | 0.2 | 0.1 | 1.9 | 4.0  | 0.5  | 1.9  | 1.1 | 0.7 | 0.8 | --   | 5.9  | 1.6 |

-- Not detected

Also observable in figure 3C (left low corner) is the presence of light lines which could appear because of the low melting point and low creep strength of lead [7]. The EDX microanalysis of the lead body (table I, P7) indicated, on the other hand, that a relatively pure and unalloyed lead (65.2 wt. %) was used for making these came since no other element with the exception of oxygen (34.8 wt. %) was detected (attributable to the lead oxide formed as a first product of the very fast interaction between the lead polished surface and the air). This fact strongly suggest that, indeed, the Monastery of Pedralbes still conserves a Medieval lead network, which could be the original or at least one replaced during the same century. Otherwise, a lead-tin alloy would be found and that probably could mean that a later removing of the lead network could have taken place. In this kind of releading, it was common to recycle removed lead networks (tin-lead alloy soldering areas included), previously melted and cast, obtaining in this way a new lead with a higher concentration of tin [11].

Figure 3D shows the SEM micrograph of a tin-lead alloy soldering point in which two clearly different phases can be observed: a tin-rich one (table I, P8) and another lead-rich one (table I, P9). These data unequivocally confirm that a tin-lead alloy was used by Medieval glaziers for joining and soldering lead came pieces. Finally, sulphur and chlorine were detected on some outer side (outdoor) fresh weathered surfaces of the specimens (table I, P10). Sulphur and chlorine are typical components of corrosion products of metals exposed to urban-marine environments such as that of Barcelona.

Four phases have been identified by XRD analysis (Fig. 4) on lead corrosion products: anglesite ( $\text{PbSO}_4$ ), lanarkite ( $\text{Pb}_2\text{O} \cdot \text{SO}_4$ ), litharge ( $\text{PbO}$ ), and metallic lead (Pb), probably dragged away from the specimen during sample preparation. These corrosion products are typical of lead exposed to an urban environment. The first step of atmospheric lead corrosion is the reaction with oxygen to form highly adherent lead oxides; then lead oxides form basic lead carbonates by reaction with atmospheric gases as

CO<sub>2</sub>. These compounds usually form a very adherent and protective layer which hinders further corrosion of the metallic substrate. However, in urban or industrial atmospheres, with a high concentration of SO<sub>2</sub>, this pollutant reacts with the carbonates, displacing CO<sub>3</sub><sup>=</sup> ions by SO<sub>4</sub><sup>=</sup> ions, and forming lead sulphates [15-17]. Lead sulphates are also very stable and protective.

An overall evaluation of the conservation state of the lead comes indicates a slight degree of corrosion, since corrosion layers observed are rather thin (30-40 μm) and the corrosion products formed play a protective role against further corrosion of lead bodies, as previous studies have shown [15, 16].

Figure 5 offers some selected SEM micrographs from fresh weathered surfaces and cross sections of the iron samples. The surface of the samples shows a porous and highly heterogeneous layer of corrosion products, with a marked relief with craters and circular pits (figure 5A). EDX microanalyses of different areas of the surface (Table II, H1-H2-H3) show the presence of oxygen, sulphur, chlorine, silicon, and calcium.

Figure 5C-D shows a cross section of the layer of corrosion products on the square-shaped saddle-bar and the T-bar pin, respectively. Both show a non-uniform corrosion layer, with pits growing into the metallic core. The thickness of such products is larger and more irregular than that of the lead samples, reaching nearly 200 μm on average. In figure 5C, corrosion products show a heterogeneous, porous, and stratified microstructure, with two different zones: a light grey area, where the only elements detected were iron (87.2 wt. %) and oxygen (Table II, H4), and a darker and very irregular zone, composed of oxygen, sulphur, calcium, and silicon, with an iron content at about 40.3 wt. %. (Table II, H5). These results could indicate that the corrosion layer formed over the iron elements is composed of iron oxides and hydroxides, and perhaps iron sulphates, whereas calcium can be attributed to putty or mortars remains. Other areas of the iron samples show a more uniform corrosion layer (Fig 5D), composed of oxygen, chlorine, calcium, silicon, and some higher contents of iron (43.4 wt. %) (Table II, H6).

XRD analysis undertaken on the iron corrosion products (figure 6) determined that they were composed of three different phases showing, as lead corrosion ones, a low degree of crystallinity. Phases detected were akaganeite [FeO(OH)], an iron hydroxide; calcite (CaCO<sub>3</sub>), and gypsum (CaSO<sub>4</sub>·2H<sub>2</sub>O). The presence of calcite could be attributed to either putty or mortar remains, while gypsum could be incorporated into the original putty or later formed from calcite as a consequence of its reaction with atmospheric SO<sub>2</sub>.

Table II. EDX microanalyses of iron samples (atomic wt. %).

| Analysis | wt. % |     |    |    |     |     |     |    |     |      |    |
|----------|-------|-----|----|----|-----|-----|-----|----|-----|------|----|
|          | O     | Na  | Mg | Al | Si  | S   | Cl  | K  | Ca  | Fe   | Mn |
| H1       | 46.4  | --  | -- | -- | 0.5 | 2.8 | 2.8 | -- | --  | 47.3 | -- |
| H2       | 42.6  | 0.3 | -- | -- | 0.7 | 2.1 | 0.7 | -- | 0.8 | 52.8 | -- |
| H3       | 54.4  | --  | -- | -- | 0.6 | 2.2 | 1.6 | -- | 0.5 | 40.7 | -- |
| H4       | 12.8  | --  | -- | -- | --  | --  | --  | -- | --  | 87.2 | -- |
| H5       | 58,1  | --  | -- | -- | 0.4 | 0.6 | --  | -- | 0.6 | 40.3 | -- |
| H6       | 53.6  | --  | -- | -- | 0.4 | --  | 2.2 | -- | 0.4 | 43.4 | -- |

-- Not detected

The presence of akaganeite ( $\beta$ -FeO·OH) instead of goethite ( $\alpha$ -FeO·OH) is a common feature of corrosion products formed on iron in chloride-rich environments. It is usually found in some irons coming from underwater archaeological findings. Akaganeite has a hollandite-type structure containing water and small amounts of chloride (about 2 wt. %). Such chloride ions stabilize the crystal lattice and cannot be removed by washing [18]. The occurrence of akaganeite is in agreement with the important amount of chloride determined through EDX microanalyses for both the fresh weathered surfaces and the cross sections. It has been proposed that the ratio Cl-/OH- is the main factor in formation of one hydroxide or another. Thus, for a ratio  $\leq 6$  only goethite is formed, while for a ratio  $\geq 8$  akaganeite is the only compound originated. In addition, both phases appear at intermediate values [19].

The presence of akaganeite is quite surprising, since important amounts of chlorine are necessary to form this compound. Seville is more than 60 km far from the sea, and therefore marine aerosols cannot be responsible for the deposition of such amount of chlorine. An explanation to the source of chlorine could be the town's harbour, which was located in the river and nearby the Cathedral. One of its quays is called the Salt Quay (Muelle de la Sal), which had an outstanding trade activity on this product (NaCl) in the past; the winds coming from this area in the river could therefore transport important amounts of salt aerosols, which were deposited on the iron elements of the nearby cathedral.

Akaganeite may pose serious difficulties for conservation of iron elements. On the one hand, it presents a higher volume than ordinary rust, which may produce mechanical damage of iron pieces. On the other hand, and under certain conditions, it could be transformed into hematite, releasing chloride ions that may continue corrosion of the metallic substrate [20].

In summary, resulting data indicate that iron supporting elements presented a higher degree of deterioration than lead comes, even though both are, obviously, different metals, with different behaviours and chronologies, coming from different buildings located in two different towns of different climatology. Nevertheless, it should be emphasised that, as a general rule, both kind of materials showed an acceptable state of conservation in spite of their ancient date of manufacture. In fact, when they were

cut, they showed a clean metallic sparkle and a fairly good state of conservation. This kind of information can be of great relevance for the work of the conservator-restorer, since a better knowledge of the characteristics, state of conservation and long term stability of these materials can determine the type and philosophy of his intervention.

In considering the most advisable cleaning treatments for these elements, it must be kept in mind that historical lead comes should never be cleaned with strongly abrasive methods. These, whether they are mechanical (hard brushes) or chemical (acidic solutions), can irreversibly remove the protective outer oxidation layer, exposing the lead matrix to new attack. Besides, since these oxidation layers do not enhance further deterioration of the lead and, on the contrary, they act as protective layers, they can be considered as patina, a natural consequence of ageing that must be preserved. Accordingly, the same principles must be applicable to all the iron elements. Adequate soft cleaning treatments and protective coatings (oxidation inhibitors) must be carefully applied in order to guarantee their longest durability and slow down the decay process. In this sense, the installation of an adequate outer protective glazing system, the so-called isothermal glazing, has since long proved to be the most effective way to preserve historical stained glass in situ and delay the inevitable degradation of the original material.

## **Conclusions**

Lead weathered comes showed a slight corrosion layer composed of anglesite ( $\text{PbSO}_4$ ), lanarkite ( $\text{Pb}_2\text{O} \cdot \text{SO}_4$ ) and litharge ( $\text{PbO}$ ). These compounds form a compact, adherent, and stable layer that behaves as a corrosion barrier. On the contrary, iron supporting elements were more intensely corroded, forming thick crusts of akaganeite [ $\text{FeO}(\text{OH})$ ], mixed with calcite ( $\text{CaCO}_3$ ) and gypsum ( $\text{CaSO}_4 \cdot 2\text{H}_2\text{O}$ ).

Keeping in mind the ancient date of manufacture and the long exposure time to weathering, the metallic elements studied present, as a general rule, a good state of conservation. This fact, and their important documentary value for the material history of the window, and therefore for the history of stained glass production in Europe, make advisable that they remain in their original place into the windows and continue to perform their primary function.

## **Acknowledgements**

The authors wish to express their gratitude to the Historical and Cultural Heritage Thematic Network (CSIC) for its professional advice. Dr M.G.-H. and Dr E.C. also acknowledge financial support provided by the CSIC-ESF through I3P postdoctoral contracts.

## References

- [1] Gillies K.J.S., Cox G.A., Decay of Medieval stained glass. Part 2. Relationship between the composition of the glass, its durability and the weathering products, *Glastech. Ber.* 61 (1988) 101-107.
- [2] Cox G.A., Heavens O.S., Newton R.G., Pollard A.M., A study of the weathering behavior of Medieval glass from York Munster, *J. Glass Studies* 21 (1979) 54-75.
- [3] Newton R.G., Fuchs D., Chemical compositions and weathering of some Medieval glasses from York Munster. Pt. 1, *Glass Tech.* 29 (1988) 43-48.
- [4] Schreiner M., Deterioration of stained Medieval glass by atmospheric attack: Pt. 1. Scanning Electron Microscopic investigations of the weathering phenomena, *Glastech. Ber* 61 (1988) 197-204.
- [5] Pérez y Jorba M., Dallas J.P., Bauer C., Deterioration of stained glass by atmospheric corrosion and microorganisms, *J. Mat. Sci.* 15 (1980) 1640-1647.
- [6] Gimeno D., Puges M., Caracterización química de la vidriera de Sant Pere i Sant Jaume (segundo cuarto del s. XIV, Monestir de Pedralbes, Barcelona), *Bol. Soc. Esp. Ceram. Vidr.* 41 (2) (2002) 225-231.
- [7] Castaño González J.G., López de Azcona C., Morcillo Linares M., Deterioration of ancient metallic elements taken from Toledo Cathedral, *Rev. Metal.* 37 (4) (2001) 519-527.
- [8] García-Heras M., Gil C., Carmona N., Villegas M.A., Weathering effects on materials from historical stained glass windows, *Mater. Construcc.* 53 (270) (2003) 21-34.
- [9] Conservation and Technology of Historical Stained Glass Windows, Proceedings of the 3rd International CVMA Forum, Fribourg, Switzerland, June 24-27 1999, *Corpus Vitrearum Medii Aevi Newsletter* 47 (2000).
- [10] Rambush, V.B., The lead comes of stained glass windows: purpose, problems and preservation procedures, *Technology and Conservation* 8 (3) (1993) 46-49.
- [11] Cortés Pizano F., Study of the Medieval lead comes used in the stained glass windows of the Monastery of Pedralbes (Barcelona), *Mater. Construcc.* 50 (259) (2000) 85-95.
- [12] Nieto Alcaide V., *Las vidrieras de la Catedral de Sevilla*, *Corpus Vitrearum Medii Aevi*, Vol. I, CSIC, Madrid, 1969.
- [13] Ainaud de Lasarte J., Vila-Grau J., Escudero Ribot M.A., Vila Delclós A., Cañellas S., Mundo A.M., *Els vitralls de la catedral de Barcelona i del Monestir de Pedralbes*, *Corpus Vitrearum Medii Aevi*, Institut d'Estudis Catalans, Barcelona, 1997.
- [14] Pugès Dorca M., Julià Capdevilla J.M., Calmell Ibáñez A., Gimeno Torrente D., Beseran Ramón P., Cortés Pizano F., *La restauració del vitrall de Sant Pere i Sant Jaume de l'església del Reial Monestir de Santa Maria de Pedralbes*, in: *Actas de las I Jornades Històriques de Historia del Vidre*, Sitges, 30 June-2 July 2000, Museu d'Arqueologia de Catalunya, Barcelona 2002, pp. 359-371.
- [15] Black, L., Allen G.C., Nature of lead patination, *Br. Corros. J.* 34 (3) (1999) 192-197.
- [16] Carradice I.A., Campbell S.A., The conservation of lead communion tokens by potentiostatic reduction, *Studies in Conservation* 39 (2) (1994) 100-106.

- [17] Melin A., Milner E.F., Sutherland C.A., Kerby R.C., Teindl H., Prengaman D., Carr D.S., Etzrodt G., Emmert R., Franz K.D., Härtner H., Nitta K., Pfaff G., Lead, in F. Habashi (Ed.), Handbook of extractive metallurgy, Wiley-VCM, Weinheim, 1997, pp. 581-639.
- [18] Šarić A., Musić S., Nomura K., Popović S., Microstructural properties of Fe-oxide powders obtained by precipitation from FeCl<sub>3</sub> solutions, Mater. Sci. Eng. B 56 (1998) 43-52.
- [19] Santana Rodríguez J.J., Santana Hernández F.J., González González J.E., XRD and SEM studies of the layer of corrosion products for carbon steel in various different environments in the province of Las Palmas (The Canary Islands, Spain), Corros. Sci. 44 (2002) 2425-2438.
- [20] Cook D.C., Van Orden A.C., Carpio J.J., Oh S.J., Atmospheric corrosion in the Gulf of México, Hyp. Interact. 113 (1998) 319-329.

## Figures

Fig. 1. Photographs showing samples analysed in this research. A and B) H-shaped lead came from the Monastery of Pedralbes (Barcelona, Spain). C) Dutchmen lead from the same location. D) Iron square-shaped saddle-bar from the Cathedral of Seville (Spain). E) Iron T-bar pin from the Cathedral of Seville (Spain).

Fig. 2. Cross section image from the iron square-shaped saddle-bar. Zone 1: cracks. Zone 2: non-homogeneous areas with non-metallic products..

Fig. 3. SEM micrographs from the lead came samples. A) Inner side surface (indoor). B) Inner H-side surface. C) Cross section showing stratified corrosion products. D) Cross section detail of a tin-lead alloy soldering area.

Fig. 4. X-ray diffractogram of a corrosion products layer from a lead came sample.

Fig. 5. SEM micrographs from iron framework supporting samples. A) Surface of the square-shaped saddle-bar. B) Cross section of the square-shaped saddle-bar. C) Cross section of the square-shaped saddle-bar showing layered corrosion products. D) Cross section of the T-bar pin showing the layer of corrosion products.

Fig. 6. X-ray diffractogram of corrosion products formed on the iron framework supporting samples.

*Artículo publicado en el Vol. 1 de las Actas de la "Conferencia Internacional de Arqueometalurgia en Europa", celebrada en Milán (Italia) los días 24, 25 y 26 de Septiembre de 2003, pp. 381-390.*

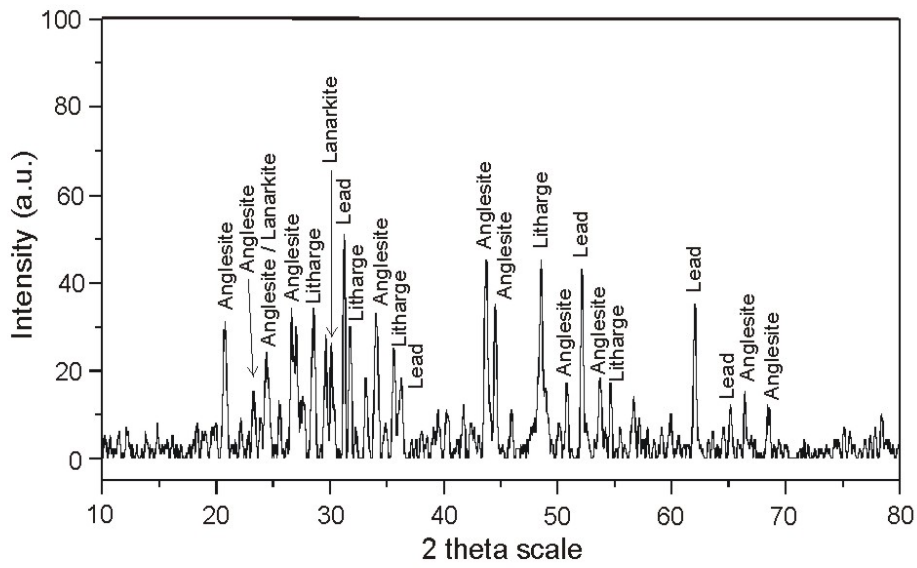


Fig. 4. X-ray diffractogram of a corrosion products layer from a lead came sample.

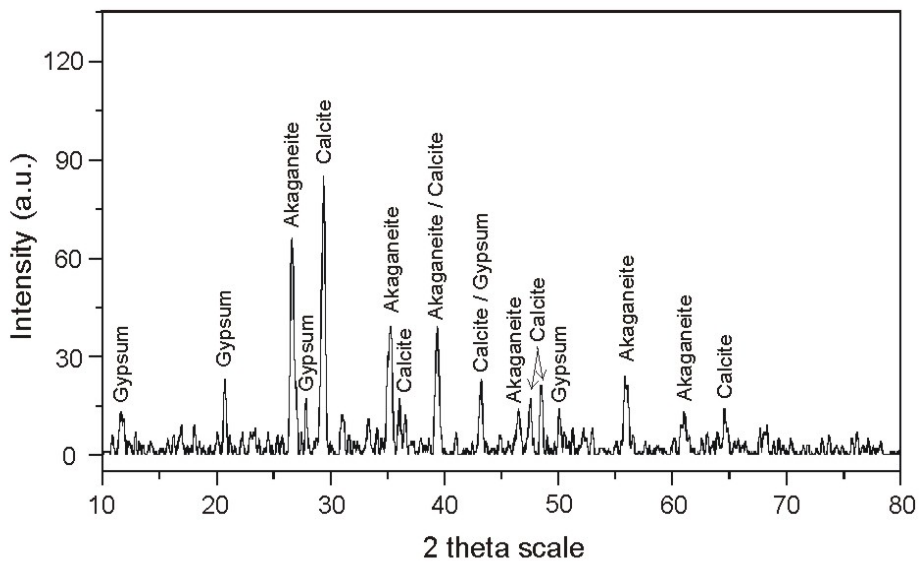


Fig. 6. X-ray diffractogram of corrosion products formed on the iron framework supporting samples.